Bottom-up Modular Synthesis of Well-Defined Oligo(arylfuran)s

Yang Chen
South China University of Technology
Tongxiang Cao
South China University of Technology
Shifa Zhu (zhusf@scut.edu.cn)
South China University of Technology https://orcid.org/0000-0001-5172-7152

Article

Keywords: oligo(arylfuran)s, oligofurans, modular synthesis

Posted Date: April 16th, 2021

DOI: https://doi.org/10.21203/rs.3.rs-385226/v1

Version of Record: A version of this preprint was published at Nature Communications on October 25th, 2021. See the published version at https://doi.org/10.1038/s41467-021-26387-5.

Bottom-up Modular Synthesis of Well-Defined Oligo(arylfuran)s

Yang Chen, Tongxiang Cao, and Shifa Zhu*

Key Laboratory of Functional Molecular Engineering of Guangdong Province, School of Chemistry and Chemical Engineering, South China University of Technology, Guangzhou 510640, China; *Correspondence: zhusf@scut.edu.cn

Oligofurans have attracted great attention in the field of materials over the last decades because of their several advantages, such as strong fluorescence, charge delocalization, and increased solubility. Although unsubstituted or alkyl substituted oligofurans have been well-established, there is an increasing demand for the development of the aryl decorated oligofuran with structural diversity and unrevealed properties. Here we report the first example of bottom-up modular construction of chemically and structurally well-defined oligo(arylfuran)s by *de novo* synthesis of α,β′-bifuran monomers and subsequent coupling reaction. Moreover, a preliminary study of the photophysical properties demonstrated that the polarity-sensitive fluorescence emission (up to 530 nm) and ultra-high Stokes shifts (up to 244 nm) could be achieved by modulating the aryl groups on the oligo(arylfuran)s. These twisted molecules constitute a new class of oligofuran backbone useful for structure−activities relationship studies and appear to be promising fluorophores.

The development of operationally straightforward and precise-effective routes for the assembly of heterocycles from simple starting materials is very important for many scientific endeavors. Furan is one of the most important five-membered heterocycles, which have been found widespread applications in bioactive pharmaceuticals,[1-3] agrochemicals[4] and functional materials.[5,6] Furthermore, the nonfused linear oligomers of furan (oligofurans, nF), can be employed as useful building block in synthetic organic chemistry[7,8] as well as a potential skeleton in material science.[9-11] In addition, oligofurans were regarded as “green” materials as furan can be directly obtained from renewable bioresources[12] and are easily biodegradable.[13] However, compared to the thio-analogues, oligothiophenes (nT), which were considered among the workhorses in the field of organic electronic materials,[14] oligofurans (nF) have been overlooked for a long time.[15-21] A decade ago, researchers have already demonstrated that oligofurans exhibited higher fluorescence, better solubility, greater rigidity, and tighter solid-state packing than the corresponding oligothiophenes. These promising advantages have spurred massive efforts toward the design and synthesis of novel oligofuran-based materials during the past decade. For example, in 1981 Kaufmann’s group have achieved the α,α-tetrafuran (α,α-4F) using the Ullmann homocoupling reaction,[15] and about twenty years later the substituted α,α-pentafuran (α,α-5F) was reported by the same group

through Negishi coupling reaction.[16] In 2010, Bendikov realized the synthesis of the α,α-nonanfuran (α,α-9F) *via* Stille coupling.[17] The longest α,α-oligofuran (16F-2C_6) bearing with adjacent C6-alkyl-substitution was synthesized by the coupling of soluble furan oligomers. (Figure 1a).[18] In addition, a unique β-substituted α,α-oligofuran (4F) was synthesized by Zhang's group *via* an elegant iterative radical tandem cyclization mediated by a Co (II)-based metalloradical catalyst.[19] Interestingly, it is also about twenty years later from Wong's seminal synthesis of the β,β-oligofuran (8F, R = SiR'$_3$),[20] an iterative cross-coupling synthesis of similar oligofuran (8F, R = Br) was achieved and revealed its 3D conformation by Paddon-Row (Figure 1b).[21] Despite of these achievements in α,α-oligofurans and β,β-oligofurans, the preparation of polyfunctional oligofurans is still challenging.

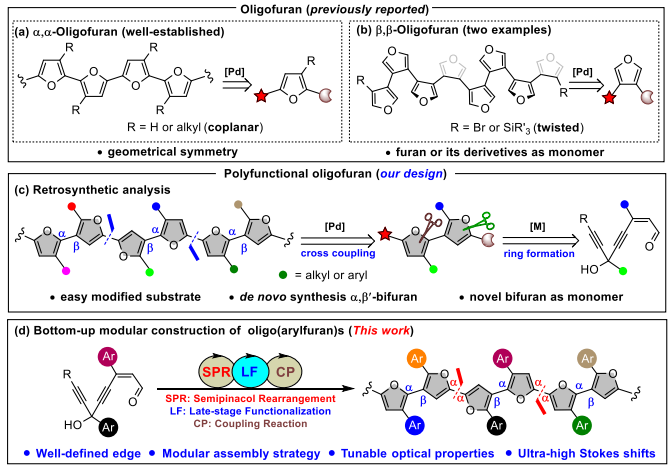

Fig. 1. Development of oligofurans. a α,α-oligofurans. **b** β,β-oligofurans. **c** retrosynthetic analysis of polyfunctional oligofuran. **d** This work: bottom-up modular synthesis of oligo(arylfuran)s.

As Bendikov observed in the 16F-6C_6 and nF-2C_6, the adjacent alkyl substituents on the C3 position have no impact on the planarity of the backbone.[18] What's more, several observations indicated the slightly twisted aryl substituents might benefit in electronic communication.[22-24] Therefore, it's reasonable to postulate that substitution of alkyl substituents with more sterically hindered aryl groups might result in slight twisted oligofurans. Importantly, the incorporation of aryl groups provides a powerful means in modulating the properties of the oligofurans *via* conjugation effect of arene. However, the limited accessibility of versatile 2,3-difunctionalized and 2,4-difunctionalized furans with suitable coupling handles and the potential competition of α-C-H bond of furan during cross coupling severely impeded efficient synthesis of aryl decorated oligofurans.[20,25] To the best of our knowledge, there is no successful report on the design and synthesis of polyaryl substituted oligofurans. In this regard, developing an efficient and reliable synthetic strategy to assemble oligo(arylfuran)s would be challenging but highly desirable.

Recently, transition metal-catalyzed cycloisomerization of enynones/enynals has become a straightforward method for the synthesis of functionalized furan.[26] Based on our previous work in this area[27-34] and also inspired by metal carbene-involved semi-pinacol rearrangement,[35-40] we envisioned

that the simple and commercially inexpensive starting material enynals might underwent a tandem cycloisomerization/selective alkynyl rearrangement/cycloisomerization reaction to furnish the desired α,β′-bifuran as monomer, which not only avoid the direct formation of the α,β-connective bond but also improve the efficiency of oligofurans assembly (Figure 1c). If such a cascade reaction is valid, it would allow the selective and straightforward introduction of different aryl groups into each furan unit of the bifurans without otherwise tedious process for introduction of the substitution. In addition, the resulting arylbifurans could serve as versatile modular building blocks in the bottom-up synthesis of chemically and structurally well-defined oligo(arylfuran)s, paving the way for deep structure-property investigation (Figure 1d).

Results

Optimization Study With obove mentioned consideration, our initial tests were set out by using aryl-enriched enynal **1-1** as the substrate for reaction condition screening. As shown in Table 1, the reactions were conducted in toluene at 60 °C. Different transition metals were tested for this transformation. The coinage metal salts, which were typically good catalysts for enynones,[29,41,42] were almost ineffective for this transformation (entries 1-3). $ZnCl_2$, another important catalyst for the cycloisomerization of enynones,[43] could not catalyze this reaction either (entry 4). Gratifyingly, the desired bifuran product **2F1** could be successfully produced in 20% yield when $(CH_3CN)_2PdCl_2$ was applied as the catalyst (entry 5). The yield could be significantly improved when $PtCl_2$ was utilized (entry 6, 63%). It has been reported that the presence of a protonic additive could often improve the reaction efficiency through assisting the protodemetalation of the vinylmetal intermediate.[44-46] As expected, the addition of isopropanol (1.1 eq.)

Table 1. Optimization of the reaction conditions[a]

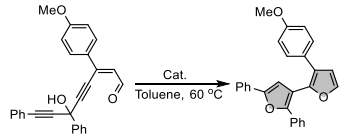

1-1 2F1

entry	cat. (mol%)	t/h	Yield[b]
1	Ph_3PAuCl (5)/AgOTf (5)	24	ND
2	$AgNTf_2$ (10)	24	trace
3	CuCl (10)	24	trace
4	$ZnCl_2$ (10)	24	ND
5	$(CH_3CN)_2PdCl_2$ (10)	24	20%
6	$PtCl_2$ (5)	24	63%
7[c]	$PtCl_2$ (5)	8	80%
8[c,d]	**$PtCl_2$ (5)**	**24**	**90%**
9[c,d]	$PtCl_2$ (1)	72	55%

[a]Unless otherwise noted, reactions performed at 0.1 M in toluene using 0.20 mmol substrate and catalyst (5 - 10 mol %) at 60 °C under a N_2 atmosphere. [b]Isolated yields. [c]1.1 equiv. of ^{i}PrOH as additive. [d][**1-1**] = 0.025 M.

as protonic additive could efficiently enhance the reaction efficiency (entry 7), which finished in shorter time (8 hours) and afforded the desired product **2F1** in higher yield (80%). Lowering the reaction concentration further improve the reaction yield to 90%(entry 9). With only 1 mol% of catalyst, the yield dropped to 55% after 72 h (entry 10).

Scope of the Investigation Having established the optimal reaction conditions (Table 1, entry 8), the substrate scope of this platinum-catalyzed tandem cycloisomerization reaction was then evaluated. As shown in Figure 2, this reaction could be successfully applied to a variety of enynals **1** with different combinations of groups R^1, R^2, and R^3. The reactions were not strongly affected by the electronic and steric properties and of groups R^1, R^2, and R^3. In most cases, the yields of bifuran products **2F** are higher than 70% yield. Different halogen atoms and methoxy group at different positions on phenyl ring were all well-tolerated. The enynal with naphthyl of R^1, however, produced the corresponding bifuran **2F11** only in 26%. Interestingly, a trifuran product **2F24** could also be assembled in 43% yield when R^2 is a furan group. In addition, the α,β′-bifuran structure was unambiguously confirmed by X-ray crystallographic analysis of **2F11**. The molecular configuration of **2F11** is noncoplanar and with large dihedral angle (66.30°) between two furan units due to the steric hindrance between the neighboring naphthalene and phenyl groups (see Supplementary Material). To extend the conjugation system of the product, we designed a bis-enynal for the synthesis of tetrafuran through double tandem cycloisomerization. Under the standard reaction conditions, the bis-enynal starting material underwent rapid and complete decomposition but did not give any desired tetrafuran product. We thought that the instability or high reactivity may arise from the two free hydroxyl groups of the starting material. Therefore, a TBS-protected bis-enynal was used instead. Under a slightly modified condition, the desired tetrafuran **4F1** could be produced in 42% yield over two steps.

As shown in Figure 2, the bifurans **2F1**-**2F25** have only one α-position open for the potential modifications, such as bromination or stannylation. Such structure will inevitably impede the following applications in the synthesis of oligofurans through cross-coupling reaction. To access the α,β′-bifuran monomer with two α-positions opening for conjugated system extension, we tried to synthesize the enyals with a terminal alkyne group. However, these molecules are unstable and are difficult to prepare. Therefore, we then turned our attention to other alternative ways. It's well known that the use of organosilyl group as a blocking group has been one of the most useful strategies in furan chemistry. Not only are they easy to introduce and remove, but they can be replaced by electrophiles *via* an *ipso*-substitution. In addition, the size of organosilyl group also has a pronounced influence on the regioselectivity for the introduction of other groups on the furan ring.[47-49] Therefore, enynals with a silicon terminus on the alkyne were then prepared for the cyclization reactions, aiming at the synthesis of silyl-substituted α,β′-bifuran. As shown in Figure 2, the cycloisomerization reactions took place smoothly under the standard reaction conditions ($PtCl_2$/^{i}PrOH). However, it's not the desired 2-silylfuran **2F-Si**, but instead a 1,2-Si migration product 3-silylfuran **2F-Si′**. It was demonstrated that functional groups such as methoxy, fluoro, nitro and nitrile could be well-tolerated under these reaction conditions, affording the C2-

unsubstituted 3-silylfurans **2F-Si′** as sole regioisomer in good yields. It is supposed that the migration might proceed through a β-silyl palatium carbene intermediate, wherein the 1,2-Si migration is kinetically favored over the 1,2-H[50-53] (See Supplementary Material for the proposed reaction mechanism). To synthesize 2-silyl-bifurans, a stepwise strategy was adopted with TBS-protected enynals as starting material. After systematic screening reaction conditions, (see the Supplementary Material), a stepwise palatium/gold relay- catalytic system was developed for the synthesis of the desired 2-silylfuran **2F-Si**. It

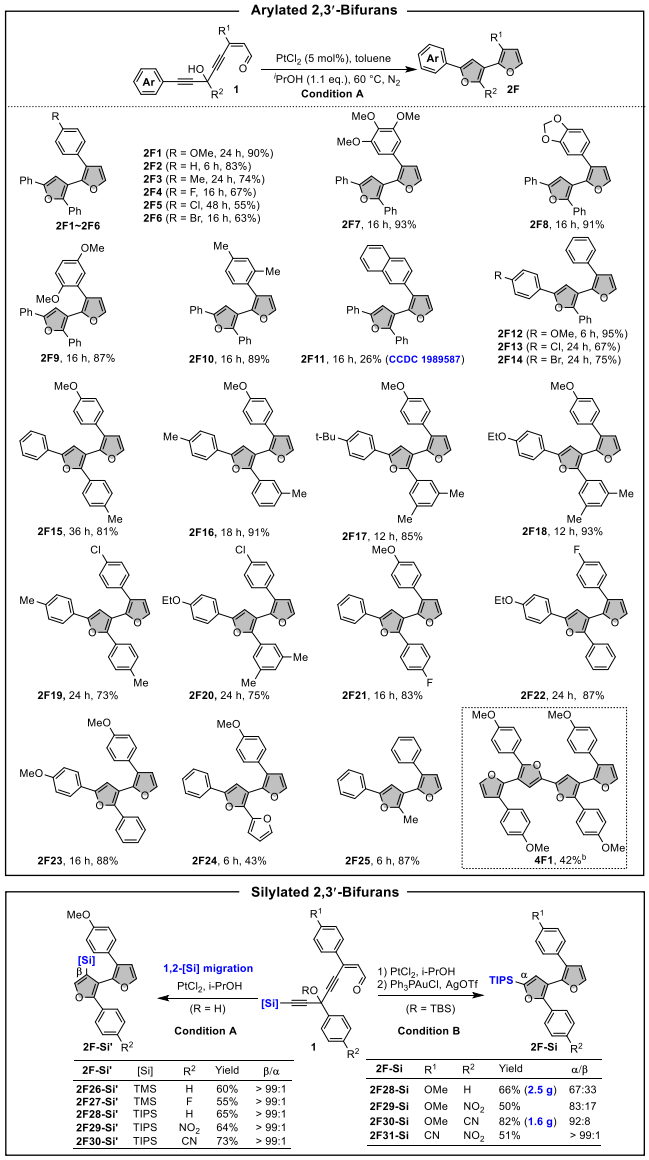

2F-Si′	[Si]	R²	Yield	β/α
2F26-Si′	TMS	H	60%	> 99:1
2F27-Si′	TMS	F	55%	> 99:1
2F28-Si′	TIPS	H	65%	> 99:1
2F29-Si′	TIPS	NO_2	64%	> 99:1
2F30-Si′	TIPS	CN	73%	> 99:1

2F-Si	R¹	R²	Yield	α/β
2F28-Si	OMe	H	66% (2.5 g)	67:33
2F29-Si	OMe	NO_2	50%	83:17
2F30-Si	OMe	CN	82% (1.6 g)	92:8
2F31-Si	CN	NO_2	51%	> 99:1

Fig. 2. Substrate scope. [a]Unless otherwise noted, the reactions were carried out in 0.2 mmol-scale under the standard conditions; [b]i) $PtCl_2$ (5 mol%), ^{i}PrOH (1.1 eq.), toluene, 60 °C; ii) $(MeCN)_4CuPF_6$ (5 mol%), toluene, 120 °C; Condition A for 1,2-[Si] migration: $PtCl_2$ (5 mol%), ^{i}PrOH (1.1 eq.), toluene, 60 °C; Condition B for the synthesis of α-silyl-bifuran: i) $PtCl_2$ (5 mol%), ^{i}PrOH (1.1 eq.), toluene, 60 °C; ii) PPh_3AuCl (5 mol%)/AgOTf (5 mol%), toluene, 90 °C. α/β-regioselectivities were measured based on H^1NMR of the crude products.

was found that a mixture of 2-silylfurans **2F-Si** and 3-silylfurans **2F-Si′** were often obtained for the electron-rich substrates, but with 2-silylfuran isomer dominated. The yields over two steps ranged from 50% to 82%. The regioselectivity of this reaction was highly dependent upon the electronic properties of the starting materials **1**. The results indicated that the more electronical deficiency of the substrates, the higher α/β-regioselectivity of the bifuran products. For example, the α/β ratio for bearing electron-deficient aryl substituents, the product α/β-regioselectivity increased significantly (**2F29-Si**, **2F30-Si**, **2F31-Si**). Especially when R^1 = CN, R^2 = NO_2, 2-silylfuran **2F31-Si** could be obtained with a selectivity of > 99/1 in 51% yield. It is noteworthy that a silyl enol ether intermediate could be isolated for the first $PtCl_2$-catalyzed step (see SI). This reaction is quite robust and can be conducted in gram scale. The present methodology constitutes a general and efficient route for the chemodivergent synthesis of silyl bifurans, which are important synthons but not easily available *via* existing methodologies.

As mentioned in the introduction part, the synthesis of oligofurans mainly relies on the transition-metal catalyzed cross coupling reactions of appropriate difunctionalized furan monomers.[17] Having established the cascade reaction as a reliable and efficient method for the *de novo* synthesis of α,β′-bifurans. We then advanced to synthesize bromo- and tin-substituted α,β′-bifuran through the bromination and stannylation reactions.[17] As shown in Figures S1 and S2, one or two bromine atoms could be selectively introduced into the backbone of bifuran with NBS as the brominating reagent and the stannylation products were easy accessed as well with Bu_3SnCl as the tin reagent (more details see Supplementary Material).

With a class of versatile modular α,β′-bifuran monomers (including bromo- and tin-bifurans) in hand, we then advanced to assemble the desired oligofurans. As shown in Figure 3, a one-step Stille coupling reaction of bromo-bifurans **2F-Br** or **2F-Br$_2$** with stannyl-bifurans **2F-Sn** gave isomerically pure tetra furans (**4F2**-**4F12**) in good to excellent yields. In addition to the monobromo-bifurans **2F-Br**, 2,3′-dibromo-bifurans could be selectively cross-coupled at 2-bromo-position, leaving 3′-bromine atom unchanged. This unique selectivity provided a good opportunity to access the 3-bromo-oligofuran family (**4F5-4F7**). The structure of bromo-tetrafuran was unambiguously confirmed by X-ray crystallographic analysis of compound **4F7**. The X-ray structure of **4F7** shows that the four furan rings are non-planar. The dihedral angle between A-ring and B-ring is 22.08°. The angle between B-ring and C-ring is 8.47° (almost coplanar), which is similar to α,α-oligofurans.[17] However, the angle between C-ring and D-ring is close to vertical (85.65°), such high torsion angle should arise from the repulsion of two aryl substituents and one bromine atom along the axial. The crystal packing shows no direct π-π interaction of the oligofuran backbone and features large interplanar distances, which is expected to suppress the fluorescence quenching and increase solid-state emissions (see the Supplementary Material). It is worth noting that there just is slightly twisted in the backbone of Ar^1-Ar^2-A-B-C ring, which is reminiscent of the organoborane acceptor-substituted polythiophene.[22] Treatment of **4F7** with 1.0 equivalent of n-BuLi produced the oligofuran **4F8** with six different aryl substituents, which is otherwise difficult to synthesize by the conventional methods. As mentioned above, the use of organosilyl group as blocking or masking

group has been the most useful in furan chemistry.[47] The silyl group will exert a profound influence upon the regioselectivity of the furan ring. For example, when 3-silyl-2,2′-dibromo-bifurans were used as coupling partners to react with stannyl-bifurans, only the bromine atom on the nonsilyl-furan is reactive for the Stille reactions. Wherein the silyl group (TMS or TIPS) served as a good masking group, and the bromine close to the bulky silyl group remained unreactive towards the standard Still coupling reactions (see **4F9**, **4F11** and **4F12**). More importantly, the masking group of silyls could be easily removed with TBAF and then the reactivity of the bromofuran will be released for the Stille-coupling reaction. For instance, upon treatment with tetrabutylammonium fluoride (TBAF) at 50 °C in THF, **4F9** underwent complete protodesilylation, affording the the corresponding tetrafuran **4F10-Br** in 63% yield, which could be utilized as important building block to access longer oligofuran (vide infra).

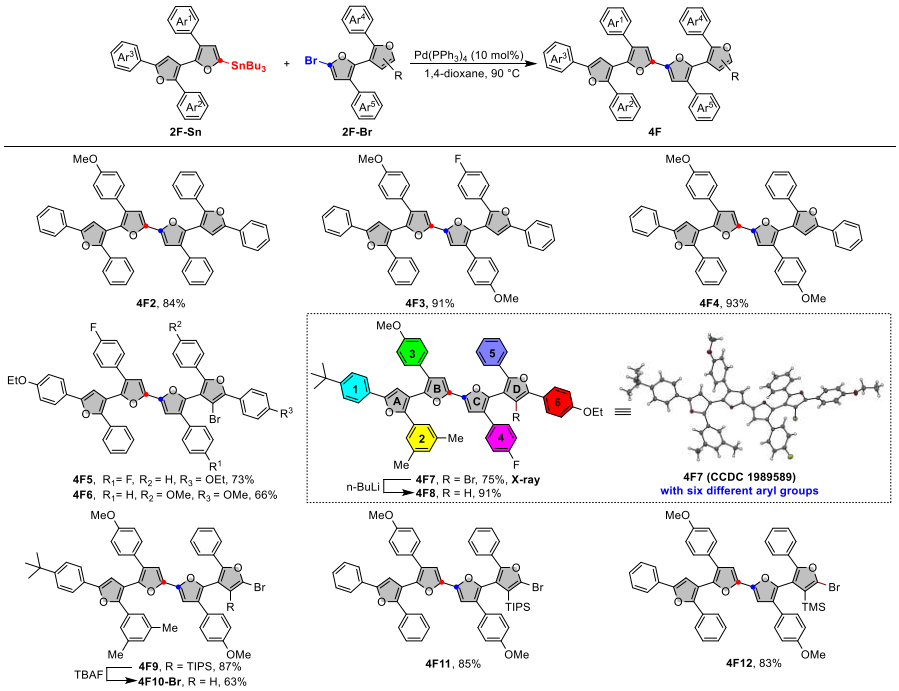

Fig. 3. Substrate scope. Stille couping conditions: $Pd(PPh_3)_4$ (10 mol%),1,4-dioxane, 90 °C, overnight.

In addition to the Stille-coupling reactions, the direct oxidative homocoupling of two bifurans through the cleavage of two C-H bonds could also be harnessed to assemble the symmetric oligofurans (Figure 4).[54] The homocoupling reaction of **2F-Si** with 1.0 equivalent of $Pd(OAc)_2$ as catalyst and oxygen (air) as the oxidant proceeded smoothly in DMSO to furnish **4F-Si$_2$** products in 36-63% yields (**4F13-Si$_2$**, **4F14-Si$_2$** and **4F15-Si$_2$**). The masking silyl groups at α-position of **4F-Si$_2$** could also be facilely removed with TBAF, affording another type of important monomer **4F13** and **4F14** with four arylfurans in good yields, as the newly released α-positions could be used as potential coupling sites for the synthesis of longer oligofurans. The structures of silyl-tetrafuran **4F-Si$_2$** were confirmed by X-ray crystallographic analysis of compound **4F13-Si$_2$** and **4F14-Si$_2$** (see the Supplementary Material). The molecular configuration of **4F13-Si$_2$** and **4F14-Si$_2$** are the same on the whole. The inside two furan rings are fully coplanar, within

the accuracy of atomic positions. The outer two furan rings are non-planar, with the dihedral angles being 51.52° for **4F13-Si$_2$** and 36.02° for **4F14-Si$_2$**, respectively, which is similar to that of **4F7** (22.08°). The above X-ray crystallographic analysis of oligo(arylfuran)s indicated that the introduction of different aryl groups would affect the conformation of oligofuran, the steric-hindrance effect between two neighbouring aryl groups disrupted the planarity of backbone of these oligo(arylfuran)s, but the coplanarity of α,α-linked furans was almost unaffected.

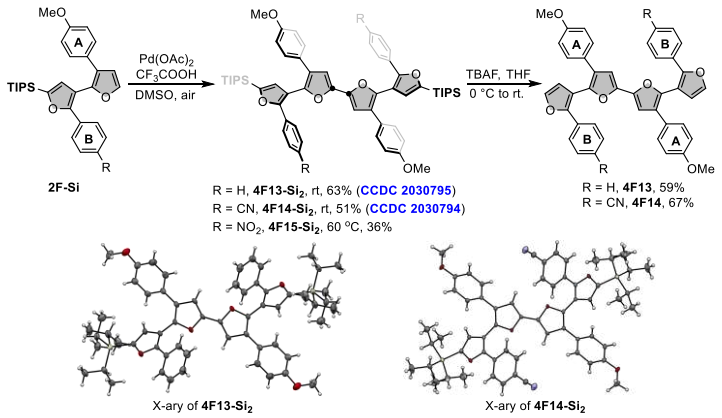

Fig. 4. Bottom-up Synthesis of Tetrafuran through Oxidative Homocoupling.

As an exhibition of superiority of the modular and programmable strategy, structurally diverse longer oligofurans were assembled quickly in a controlled and designed manner by choosing different bifuran and tetrafuran as coupling partners (Figure 5). For example, a double Stille coupling reaction of **2F1-Sn** and **2F32-Br$_2$** under catalysis of Pd(PPh$_3$)$_4$ successfully afforded isomerically pure sexifuran **6F** in 75% isolated yield. In the same manner, functionalized tetrafuran could be used as Pd(PPh$_3$)$_4$, the decafuran **10F** with ten arylfuran units could be assembled successfully in 40% yield over two steps.

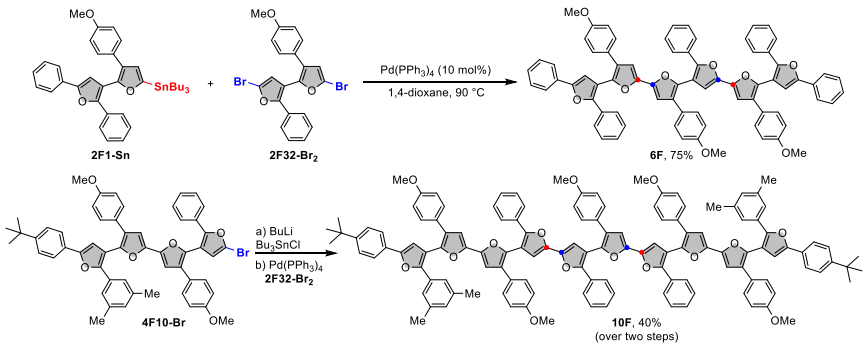

Fig. 5. Bottom-up Synthesis of Sexifuran and Decafuran.

So far, the photophysical properties of oligofurans are only limited to α,α-oligofurans and β,β-oligofurans.[15-21] The UV/Vis absorption and emission spectra of the representative bifuran (**2F**), tetrafuran (**4F**), sexifuran (**6F**) and decafuran (**10F**) in solutions were then characterized and shown in Table 2 and Figure 6. The absorption and emission maxima of these complexes vary from 263 nm to 332 nm, and

430 nm to 530 nm, respectively, depending on the number of furan units and aryl groups. To the general trends, the absorption was red-shifted as the number of furan units increased, such as the λ_{max} of **10F** was bathochromically shifted by 69 nm compared to **2F1** (Table 2). But the aryl substituents of oligofurans had much more impact on the photophysical properties than the number of furan units. Oligofurans **4F1**, **4F2**, **4F13**, in which all the aryl groups only having EDGs, show blue-shifts in the λ_{max} relative to push-pull oligofuran **4F14**. The organosilyl groups on the terminus of the oligofuran have little effect on the UV absorption, such as the **4F13** (271 nm) and **4F13-Si$_2$** (265 nm). Collectively, there was no obvious linear correlation as the increment of number of furan, which indicated that the planarity is disrupted.[17]

Table 2. Basic Photophysical Properties of Oligo(arylfuran)s.

Compound	λ_{max}[a] (nm)	λ_{em}[b] (nm)	$\Delta\lambda$[c] (nm)	$\Delta\nu$[d] (cm^{-1})
2F1	263	405	142	13331
4F1	286	430	144	11709
4F2	262	474	212	17070
4F13	271	437	166	14017
4F13-Si$_2$	265	469	204	16413
4F14	318	519	201	12179
4F14-Si$_2$	313	530	217	13081
6F	276	474	198	15135
10F	332	476	144	9112

[a]Absorption maximum. [b]Emission maximum. [c]Stokes shift, $\Delta\lambda = \lambda em - \lambda max$. [d]$\Delta\nu = 1/\lambda max - 1/\lambda em$. Concentration: 10 μM; λex= 365 nm.

The solutions of these oligo(aryl)furans in DCM were highly fluorescent (Figure 6c). The emission wavelengths can effectively cover the whole visible light range from 400 to 700 nm. The maximum fluorescence emission wavelength of bifuran **2F1** was located at 405 nm. With increasing the number of furan units, the fluorescence emission wavelength has a significant red shift, such as **4F13-Si$_2$** (469 nm). But the shift of the fluorescence emission peak will not have larger red shift when the number of furan rings continues to increase to 6 or 10. This observation is completely different with those non-substituted α,α-oligofurans in the literature.[17] The reason for this phenomenon may be that the oligo(arylfuran)s are not a large conjugation system because of the introduction of aryl groups into the oligofuran backbones, as exemplified by the X-ray structures of **4F7**, **4F13-Si$_2$**, **4F14-Si$_2$**. Oligofuran **4F14** showed relatively strong emission in solution and has a relatively longer emission (519 nm) than other oligofurans. We postulated that this redshift might result from the presence of the para-CN group at the B phenyl group, which augments the efficiency of the CT process. Interestingly, the introduction of silyl group at the α terminus (**4F14-Si$_2$**) will make the emission wavelengths further shift to 530 nm,[55] which is the most red-shifted emission. These results indicated that the strategy of combining the push-pull design and silyl effect is a viable one for red- shifting the absorption and emission band of oligofurans, which enable this protocol to prepare near-infrared oligo(arylfuran)s.

Additionally, the fluorescence spectroscopic behavior of **4F14**, **4F14-Si2** were also investigated in the solid-state. The emission spectra of the solids were shown in Figure S5 (see the Supplementary Material for more details). Generally, the emission bands are nonsymmetric and very broad whereby the band broadening of **4F14-Si2** is significantly more pronounced. Similarly, analysis of the fluorescence spectra

of bisilyl substituted tetrafuran derivatives **4F14-Si2** demonstrates that silyl substitution causes emission maxima to shift to longer wavelengths by 93 nm.

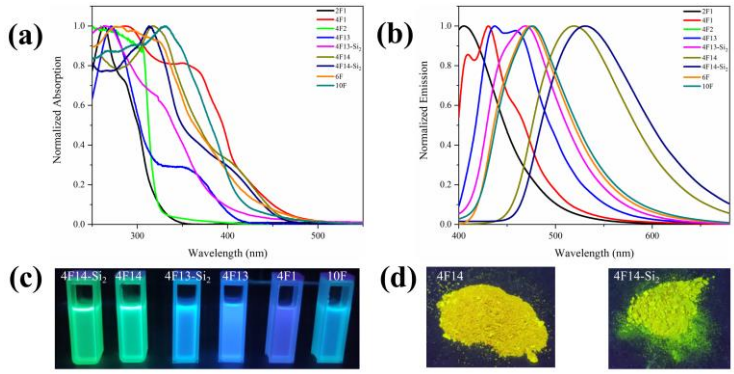

Fig. 6. (a) Absorption spectra of representative oligo(arylfuran)s in DCM (Concentration: 10 μM). (b) Emission spectra in DCM (λex =365 nm, Concentration: 10 μM). (c) Picture of oligo(arylfuran)s in DCM under UV light irradiation (365 nm). (d) Fluorescence image (powder, λex =365 nm).

Intrigued by the strongly red-shifted emission, we also undertook solvochromicity studies with **4F13-Si$_2$**, **4F14**, **4F14-Si$_2$** and **10F** to scrutinize the effect of the solvent environment on their absorption and emission properties (Figure S6, Supplementary Material). It is visually evident that compounds **4F14** and **4F14-Si$_2$** exhibited a positive emission solvatochromism, their emission is shifted bathochromically with increasing solvent polarity (cyclohexane to methanol), the corresponding emission spans the wavelengths from 502 to 559 nm and from 489 nm to 549 nm respectively, covering blue, green, yellow, and orange region of visible spectrum (Figures 5a and 5b). Such strong solvatochromism occurs due to a combination of intramolecular charge transfer (TICT) and dipole–solvent interactions in solutions.[56] On the contrary, the absorption of **4F14-Si$_2$** exhibited little change on changing the solvent polarity (Table S2 and Figure S6 in Supplementary Material). The absorption maximum of **4F14-Si$_2$** only changed from 324 nm to 328 nm by increasing the solvent polarity. Thus the solvent dependence of the emission shows that the excited state is stabilized in more polar solvents, which is due to an intramolecular charge transfer.[57]

To our delight, most of the oligofurans complexes exhibit large Stokes shifts,[58-60] ranging from 142 nm to 217 nm (Table 2). Analysis of the Stokes shift values in different solvents for the investigated molecules showed large Stokes shift values for most compounds. The large increase in the values of the Stokes shift followed the increase in the solvent polarity, as demonstrated by the compounds **4F13-Si$_2$**, **4F14**, **4F14-Si$_2$**, in cyclohexane, toluene, 1,4-Dioxane, THF, DCM, chloroform, acetonitrile, DMF, DMSO, MeOH with values in the range of 174 – 244 nm. Moreover, **4F14** possesses a super large Stokes shift, in excess of 240 nm (Δλ), with an associated energy value (Δν) of ~15000 cm^{-1}, which is very useful for small organic fluorophores,[61,62] especially for their imaging applications.[63-65]

Representative plots containing the absorption and emission spectra of compound **4F14** in DMF **(**Figure 7c**)** and compound **4F14-Si$_2$** in DMSO (Figure 7d) are presented in Figure 7. As shown in the plots, large Stokes shifts of 244 nm (**4F14**) and 231 nm (**4F14-Si$_2$**) were realized, largely avoiding the overlap of the absorption spectrum and emission spectrum. Minimal spectral overlap between absorption and emission distinguishes oligo(arylfuran)s from the reported α,α-oligofurans and β,β-oligofurans.[17,18,21] This property is highly demanded for fluorescence probes as it prevents the self-absorption or "inner-filter" effect to increase the signal to noise ratio for fluorescence imaging.[66]

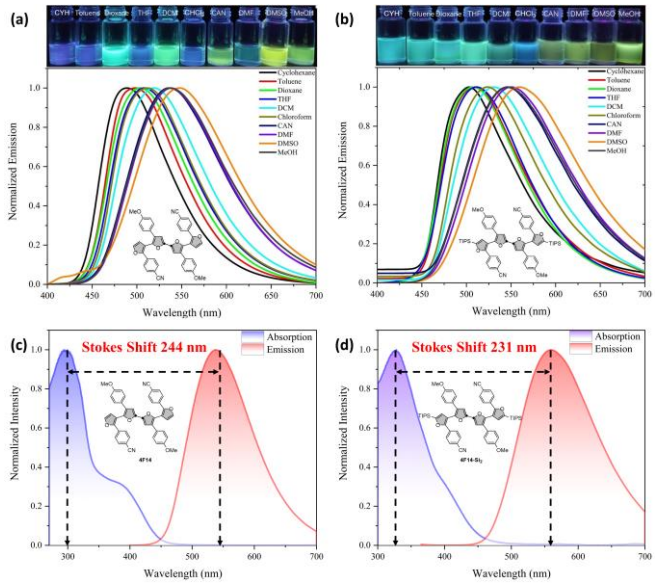

Fig. 7. Fluorescence spectra of (a) **4F14** and (b) **4F14-Si$_2$** in solvents of different polarity (THF, tetrahydrofuran; DCM, dichloromethane; CAN, acetonitrile; DMF, N,N- dimethylformamide; DMSO, dimethyl sulfoxide) under 365 nm excitatation. Concentration: 10 μM; Normalized absorption and emission spectra of (c) **4F14** in DMF and (d) **4F14-Si$_2$** in DMSO showing the overlap region.

All the synthesized oligo(arylfuran)s exhibit excellent solubility in common organic solvents, such as toluene, chloroform, DCM, and THF. Tetrafurans are stable in powdered form and even as a DCM solution when exposed to air (including moisture air) at room temperature for up to at least a few weeks. The simple furan derivatives containing electron-rich groups reported in the previous literature are usually unstable with respect to a combination of light and oxygen, are known to react with singlet oxygen to form unsaturated esters or decompose via ring opening of furan endoperoxide.[25,67] The stability of the series of oligo(arylfuran)s was verified by TGA measurement (Figure S10, Supplementary Material) and a parameter of T_{d10} (10% weight-loss temperature)[68] is used to describe the thermal durability of these compounds (see Table S3 in Supplementary Material). The TGA curves of oligo(arylfuran)s indicated that they remained almost unchangeable when the temperature is below 230 °C and the T_{d10} values were found to range from 267 to 457 °C. The push-pull derivatives **4F14** and **4F14-Si$_2$** show higher thermal stability compared with other oligo(arylfuran) compounds. It is worth mentioning that the T_{d10} value for the

4F14 can still reach 414 °C even in the atmosphere of air, which suggests that it can satisfy the stability requirements for applications in organic electronic devices.

Discussion

In summary, we have developed the first bottow-up modular construction of chemically and struturally well-difined multiaryl-substituted oligofurans *via* a platinum-catalyzed *de novo* systhesis of bifuran monomers and palladium-catalyzed cross-coupling reaction. It is worth mentioning that tetrafuran **4F8** with six different phenyl substituents could be synthesized by this means. Single-crystal X-ray analyses revealed that the steric-hindrance effect between aryl groups and neighbouring furan rings distrupted the planarity of backbone of these oligo(arylfuran)s, but there still have manipulating space in acheiving slight twist oligo(arylfuran)s in terms of the crystal date of **4F7**. These twisted oligo(arylfuran)s exhibit excellent solubility in common organic solvents (toluene, chloroform, DCM, and THF) and the high stability towards heat, oxygen and moisture. More importantly, the photophysical properties could also be well-modulated by installing different aryl groups, such as tunable and polarity-sensitive fluorescence emission and ultra-high Stokes shifts up to 244 nm (15426 cm^{-1}). The modular assemblied oligo(arylfuran)s generated by varying the aryl substituents in the resulting oligomers together with rapid characterization methods will provide us a way to the accelerated investigation on structure property relationships. Further investigations of the application of these oligo(arylfuran)s are currently in progress in our laboratory.

Methods

General procedure I: Under nitrogen atmosphere, to a solution of enynals **1** (0.2 mmol) in dry toluene (0.025 M), $PtCl_2$(0.05 eq, 2.7 mg) and ^{i}PrOH (1.1 eq, 13.2 mg) were added. The reaction mixture was then heated to a temperature of 60 °C and stirred for 6 - 48 hours. After the reaction was completed, the reaction mixture was filtered through short silica gel, and then the solvent was removed under reduced pressure. The bifuran product was purified by flash column chromatography (silica gel, petroleum ether/AcOEt = 100:1) to yield **2F**.

General procedure II:

Under nitrogen atmosphere, to a solution of enynals **1** (0.2 mmol) in dry toluene (0.025 M), $PtCl_2$ (0.05 eq, 2.7 mg) and ^{i}PrOH (1.1 eq, 13.2 mg) were added. The reaction mixture was then heated to a temperature of 60 °C and stirred for 6-48 hours. After the reaction was completed, the reaction mixture was filtered through short silica gel, and then the solvent was removed under reduced pressure. The bifuran product was purified by flash column chromatography (silica gel, petroleum ether/AcOEt = 100:1) to yield **S1**.

Under nitrogen atmosphere, to a solution of **S1** (0.1 mmol) in dry toluene (0.1 M), $Au(PPh_3)Cl$ (5 mol%, 2.4 mg) and AgOTf (5 mol%, 1.2 mg) were added. The reaction mixture was then heated to a temperature of 90 °C and stirred for 12 - 24 h. After the reaction was completed, the reaction mixture was filtered

through short silica gel, and then the solvent was removed under reduced pressure. The bifuran product was purified by flash column chromatography (silica gel, petroleum ether/AcOEt = 10:1) to yield **2F-Si**.

Data availability

The data for X-ray crystallographic structure **2F11**, **4F7**, **4F13-Si$_2$**, **4F14-Si$_2$** has been deposited in the Cambridge Crystallographic Database Center under accession number CCDC: 1989587, 1989589, 2030795, 2030794.

References

1. Palnitkar, S. S.; Bin, B.; Jimenez, L. S.; Morimoto, H.; Williams, P. G.; Paul-Pletzer, K.; Parness, J. [3H]Azidodantrolene: synthesis and use in identification of a putative skeletal muscle dantrolene binding site in sarcoplasmic reticulum. *J. Med. Chem.* **42**, 1872-1880 (1999).
2. Sperry, J. B.; Wright, D. L. Furans, thiophenes and related heterocycles in drug discovery. *Curr. Opin. Drug Discovery Dev.* **8**, 723-740 (2005).
3. Hasegawa, F.; Niidome, K.; Migihashi, C.; Murata, M.; Negoro, T.; Matsumoto, T.; Kato, K.; Fujii, A. Discovery of furan-2-carbohydrazides as orally active glucagon receptor antagonists. *Bioorg. Med. Chem. Lett.* **24**, 4266-4270 (2014).
4. Sagratini, G.; Angeli, P.; Buccioni, M.; Gulini, U.; Marucci, G.; Melchiorre, C.; Leonardi, A.; Poggesi, E.; Giardina, D. Synthesis and α(1)-adrenoceptor antagonist activity of derivatives and isosters of the furan portion of (+)-cyclazosin. *Bioorg. Med. Chem. Lett.* **15**, 2334-2345 (2007).
5. Xiong, Y.; Tao, J.; Wang, R.; Qiao, X.; Yang, X.; Wang, D.; Wu, H.; Li, H. A Furan-Thiophene-Based Quinoidal Compound: A New Class of Solution-Processable High-Performance π-Type Organic Semiconductor. *Adv. Mater.* **28**, 5949-5953 (2016).
6. Woo, C. H.; Beaujuge, P. M.; Holcombe, T. W.; Lee, O. P.; Frechet, J. M. Incorporation of furan into low band-gap polymers for efficient solar cells. *J. Am. Chem. Soc.* **132**, 15547-15549 (2010).
7. Gidron, O.; Shimon, L. J.; Leitus, G.; Bendikov, M. Reactivity of long conjugated systems: selectivity of Diels-Alder cycloaddition in oligofurans. *Org. Lett.* **14**, 502-505 (2012).
8. Gadakh, S.; Shimon, L. J. W.; Gidron, O. Regioselective Transformation of Long π-Conjugated Backbones: From Oligofurans to Oligoarenes. *Angew. Chem. Int. Ed.* **56**, 13601-13605 (2017).
9. Bunz, U. H. α-oligofurans: molecules without a twist. *Angew. Chem. Int. Ed.* **49**, 5037-5040 (2010).
10. Gidron, O.; Dadvand, A.; Sheynin, Y.; Bendikov, M.; Perepichka, D. F. Towards "green" electronic materials. α-Oligofurans as semiconductors. *Chem. Commun.* **47**, 1976-1978 (2011).
11. Gidron, O.; Bendikov, M. α-Oligofurans: an emerging class of conjugated oligomers for organic electronics. *Angew. Chem. Int. Ed.* **53**, 2546-2555 (2014).
12. Binder, J. B.; Raines, R. T. Simple chemical transformation of lignocellulosic biomass into furans for fuels and chemicals. *J. Am. Chem. Soc.* **131**, 1979-1985 (2009).

13. Koopman, F.; Wierckx, N.; de Winde, J. H.; Ruijssenaars, H. J. Identification and characterization of the furfural and 5-(hydroxymethyl)furfural degradation pathways of Cupriavidus basilensis HMF14. *Proc. Natl. Acad. Sci. USA* **107**, 4919-4924 (2010).
14. Park, K. H.; Kim, W.; Yang, J.; Kim, D. Excited-state structural relaxation and exciton delocalization dynamics in linear and cyclic π-conjugated oligothiophenes. *Chem. Soc. Rev.* **47**, 4279-4294 (2018).
15. Kauffmann, T.; Lexy, H.; Kriegesmann, R. Übergangsmetallaktivierte organische Verbindungen, IX: Synthese von Polyfuranen durch metallorganische oxidative Kupplung. *Chem. Ber.* **114**, 3667-3673 (1981).
16. Kauffman, J. M.; Moyna, G. Novel fluorescent quater- and quinquifurans: Syntheses and photophysical properties. *J. Heterocycl. Chem.* **39**, 981-988 (2002).
17. Gidron, O.; Diskin-Posner, Y.; Bendikov, M. α-oligofurans. *J. Am. Chem. Soc.* **132**, 2148-50 (2010).
18. Jin, X. H.; Sheberla, D.; Shimon, L. J.; Bendikov, M. Highly coplanar very long oligo(alkylfuran)s: a conjugated system with specific head-to-head defect. *J. Am. Chem. Soc.* **136**, 2592-2601 (2014).
19. Cui, X.; Xu, X.; Wojtas, L.; Kim, M. M.; Zhang, X. P. Regioselective synthesis of multisubstituted furans via metalloradical cyclization of alkynes with α-diazocarbonyls: construction of functionalized α-oligofurans. *J. Am. Chem. Soc.* **134**, 19981-19984 (2012).
20. Song, Z. Z.; Wong, H. N. C. Regiospecific Synthesis of Furan-3,4-Diyl Oligomers Via Palladium-Catalyzed Self-Coupling of Organoboroxines. *J. Org. Chem.* **59**, 33-41 (1994)
21. Fallon, T.; Willis, A. C.; Rae, A. D.; Paddon-Row, M. N.; Sherburn, M. S. β-Oligofurans. *Chem. Sci.* **3**, 2133-2137 (2012).
22. Li, H.; Sundararaman, A.; Venkatasubbaiah, K.; Jakle, F. Organoborane acceptor-substituted polythiophene via side-group borylation. *J. Am. Chem. Soc.* **129**, 5792-5793 (2007).
23. Holcombe, T. W.; Woo, C. H.; Kavulak, D. F.; Thompson, B. C.; Frechet, J. M. All-polymer photovoltaic devices of poly(3-(4-n-octyl)-phenylthiophene) from Grignard Metathesis (GRIM) polymerization. *J. Am. Chem. Soc.* **131**, 14160-14161 (2009).
24. Ruseckas, A.; Namdas, E. B.; Ganguly, T.; Theander, M.; Svensson, M.; Andersson, M. R.; Inganas, O.; Sundstrom, V. Intra- and interchain luminescence in amorphous and semicrystalline films of phenyl-substituted polythiophene. *J. Phys. Chem. B* **105**, 7624-7631 (2001).
25. Politis, J. K.; Nemes, J. C.; Curtis, M. D. Synthesis and characterization of regiorandom and regioregular poly(3-octylfuran). *J. Am. Chem. Soc.* **123**, 2537-2547 (2001).
26. Gulevich, A. V.; Dudnik, A. S.; Chernyak, N.; Gevorgyan, V. Transition metal-mediated synthesis of monocyclic aromatic heterocycles. *Chem. Rev* **113**, 3084-3213 (2013).
27. Ma, J.; Zhang, L.; Zhu, S. Enynal/Enynone: A Safe and Practical Carbenoid Precursor. *Curr. Org. Chem.* **20**, 102-118 (2015).
28. Chen, L. F.; Chen, K.; Zhu, S. F. Transition-Metal-Catalyzed Intramolecular Nucleophilic Addition of Carbonyl Groups to Alkynes. *Chem* **4**, 1208-1262 (2018).

29. Chen, L.; Liu, Z.; Zhu, S. Donor- and acceptor-enynals/enynones. *Org. Biomol. Chem.* **16**, 8884-8898 (2018).
30. Ma, J.; Jiang, H.; Zhu, S. NHC-AuCl/selectfluor: a highly efficient catalytic system for carbene-transfer reactions. *Org. Lett.* **16**, 4472-4475 (2014).
31. Luo, H.; Chen, K.; Jiang, H.; Zhu, S. A Route to Polysubstituted Aziridines from Carbenes and Imines through a Nondiazo Approach. *Org. Lett.* **18**, 5208-5211 (2016).
32. Zhu, D.; Ma, J.; Luo, K.; Fu, H.; Zhang, L.; Zhu, S. Enantioselective Intramolecular C-H Insertion of Donor and Donor/Donor Carbenes by a Nondiazo Approach. *Angew. Chem. Int. Ed.* **55**, 8452-8456 (2016).
33. Zhu, D.; Chen, L.; Zhang, H.; Ma, Z.; Jiang, H.; Zhu, S. Highly Chemo- and Stereoselective Catalyst-Controlled Allylic C-H Insertion and Cyclopropanation Using Donor/Donor Carbenes. *Angew. Chem. Int. Ed.* **57**, 12405-12409 (2018).
34. Zhu, D.; Chen, L.; Fan, H.; Yao, Q.; Zhu, S. Recent progress on donor and donor-donor carbenes. *Chem. Soc. Rev.* **49**, 908-950 (2020).
35. Couty, S.; Meyer, C.; Cossy, J. Diastereoselective gold-catalyzed cycloisomerizations of ene-ynamides. *Angew. Chem. Int. Ed.* **45**, 6726-6730 (2006).
36. Kirsch, S. F.; Binder, J. T.; Crone, B.; Duschek, A.; Haug, T. T.; Liebert, C.; Menz, H. Catalyzed tandem reaction of 3-silyloxy-1,5-enynes consisting of cyclization and pinacol rearrangement. *Angew. Chem. Int. Ed.* **46**, 2310-2313 (2007).
37. Li, G.; Zhang, L. Gold-catalyzed intramolecular redox reaction of sulfinyl alkynes: efficient generation of α-oxo gold carbenoids and application in insertion into R--CO bonds. *Angew. Chem. Int. Ed.* **46**, 5156-9 (2007).
38. Yeom, H. S.; Lee, Y.; Jeong, J.; So, E.; Hwang, S.; Lee, J. E.; Lee, S. S.; Shin, S. Stereoselective one-pot synthesis of 1-aminoindanes and 5,6-fused azacycles using a gold-catalyzed redox-pinacol-Mannich-Michael cascade. *Angew. Chem. Int. Ed.* **49**, 1611-1614 (2010).
39. Miura, T.; Funakoshi, Y.; Morimoto, M.; Biyajima, T.; Murakami, M. Synthesis of enaminones by rhodium-catalyzed denitrogenative rearrangement of 1-(N-sulfonyl-1,2,3-triazol-4-yl)alkanols. *J. Am. Chem. Soc.* **134**, 17440-17443 (2012).
40. Wang, T.; Shi, S.; Hansmann, M. M.; Rettenmeier, E.; Rudolph, M.; Hashmi, A. S. Synthesis of highly substituted 3-formylfurans by a gold(I)-catalyzed oxidation/1,2-alkynyl migration/cyclization cascade. *Angew. Chem. Int. Ed.* **53**, 3715-3719 (2014).
41. Yang, J. M.; Li, Z. Q.; Li, M. L.; He, Q.; Zhu, S. F.; Zhou, Q. L. Catalytic B-H Bond Insertion Reactions Using Alkynes as Carbene Precursors. *J. Am. Chem. Soc.* **139**, 3784-3789 (2017).
42. Peng, H.; Wan, Y.; Zhang, Y.; Deng, G. Synthesis of 2-alkenylfurans via a Ag(I)-catalyzed tandem cyclization/cross-coupling reaction of enynones with iodonium ylides. *Chem. Commun.* **56**, 1417-1420 (2020).

43. Vicente, R.; Gonzalez, J.; Riesgo, L.; Gonzalez, J.; Lopez, L. A. Catalytic generation of zinc carbenes from alkynes: zinc-catalyzed cyclopropanation and Si-H bond insertion reactions. *Angew. Chem. Int. Ed.* **51**, 8063-8067 (2012).
44. Staben, S. T.; Kennedy-Smith, J. J.; Huang, D.; Corkey, B. K.; Lalonde, R. L.; Toste, F. D. Gold(I)-catalyzed cyclizations of silyl enol ethers: application to the synthesis of (+)-lycopladine A. *Angew. Chem. Int. Ed.* **45**, 5991-5994 (2006).
45. Kirsch, S. F.; Binder, J. T.; Crone, B.; Duschek, A.; Haug, T. T.; Liebert, C.; Menz, H. Catalyzed tandem reaction of 3-silyloxy-1,5-enynes consisting of cyclization and pinacol rearrangement. *Angew. Chem. Int. Ed.* **46**, 2310-2313 (2007).
46. Hashmi, A. S.; Yang, W.; Rominger, F. Gold(I)-catalyzed formation of benzo[b]furans from 3-silyloxy-1,5-enynes. *Angew. Chem. Int. Ed.* **50**, 5762-5765 (2011).
47. Keay, B. A. Synthesis of multi-substituted furan rings: the role of silicon. *Chem. Soc. Rev.* **28**, 209-215 (1999).
48. Song, Z. Z.; Ho, M. S.; Wong, H. N. C. Regiospecific Synthesis of 3,4-Disubstituted Furans .7. Synthesis and Reactions of 3,4-Bis(Trimethylsilyl)Furan - Diels-Alder Cycloaddition, Friedel-Crafts Acylation, and Regiospecific Conversion To 3,4-Disubstituted Furans. *J. Org. Chem.* **59**, 3917-3926 (1994).
49. Matsui, K.; Shibuya, M.; Yamamoto, Y. Ruthenium-Catalyzed Transfer Oxygenative [2+2+1] Cycloaddition of Silyldiynes Using Nitrones as Adjustable Oxygen Atom Donors. Synthesis of Bicyclic 2-Silylfurans. *Acs Catalysis.* **5**, 6468-6472 (2015).
50. Allegretti, P. A.; Ferreira, E. M. Generation of α,β-unsaturated platinum carbenes from homopropargylic alcohols: rearrangements to polysubstituted furans. *Org. Lett.* **13**, 5924-5927 (2011).
51. Song, L.; Feng, Q.; Wang, Y.; Ding, S.; Wu, Y. D.; Zhang, X.; Chung, L. W.; Sun, J. Ru-Catalyzed Migratory Geminal Semihydrogenation of Internal Alkynes to Terminal Olefins. *J. Am. Chem. Soc.* **141**, 17441-17451 (2019).
52. Shiroodi, R. K.; Vera, C. I.; Dudnik, A. S.; Gevorgyan, V. Synthesis of furans and pyrroles via migratory and double migratory cycloisomerization reactions of homopropargylic aldehydes and imines. *Tetrahedron Lett.* **56**, 3251-3254 (2015).
53. Feng, Q.; Wu, H.; Li, X.; Song, L.; Chung, L. W.; Wu, Y.-D.; Sun, J. Ru-Catalyzed Geminal Hydroboration of Silyl Alkynes via a New gem-Addition Mechanism. *J. Am. Chem. Soc.* **142**, 13867-13877 (2020).
54. Li, N. N.; Zhang, Y. L.; Mao, S.; Gao, Y. R.; Guo, D. D.; Wang, Y. Q. Palladium-catalyzed C-H homocoupling of furans and thiophenes using oxygen as the oxidant. *Org. Lett.* **16**, 2732-2735 (2014).
55. Maeda, H.; Maeda, T.; Mizuno, K. Absorption and fluorescence spectroscopic properties of 1- and 1,4-silyl-substituted naphthalene derivatives. *Molecules* **17**, 5108-5125 (2012).

56. Cheruku, P.; Huang, J. H.; Yen, H. J.; Iyer, R. S.; Rector, K. D.; Martinez, J. S.; Wang, H. L. Tyrosine-derived stimuli responsive, fluorescent amino acids. *Chem. Sci.* **6**, 1150-1158 (2015).
57. Park, Y. I.; Kuo, C. Y.; Martinez, J. S.; Park, Y. S.; Postupna, O.; Zhugayevych, A.; Kim, S.; Park, J.; Tretiak, S.; Wang, H. L. Tailored electronic structure and optical properties of conjugated systems through aggregates and dipole-dipole interactions. *ACS Appl. Mater. Interfaces* **5**, 4685-4695 (2013).
58. Sakunkaewkasem, S.; Petdum, A.; Panchan, W.; Sirirak, J.; Charoenpanich, A.; Sooksimuang, T.; Wanichacheva, N. Dual-Analyte Fluorescent Sensor Based on [5]Helicene Derivative with Super Large Stokes Shift for the Selective Determinations of Cu^{2+} or Zn^{2+} in Buffer Solutions and Its Application in a Living Cell. *ACS Sens.* **3**, 1016-1023 (2018).
59. Hong, J. X.; Zhou, E. B.; Gong, S. Y.; Feng, G. Q. A red to near-infrared fluorescent probe featuring a super large Stokes shift for light-up detection of endogenous H_2S. *Dyes Pigm.* **160**, 787-793 (2019).
60. Dhara, A.; Sadhukhan, T.; Sheetz, E. G.; Olsson, A. H.; Raghavachari, K.; Flood, A. H. Zero-Overlap Fluorophores for Fluorescent Studies at Any Concentration. *J. Am. Chem. Soc.* **142**, 12167-12180 (2020).
61. Araneda, J. F.; Piers, W. E.; Heyne, B.; Parvez, M.; McDonald, R. High Stokes shift anilido-pyridine boron difluoride dyes. *Angew. Chem. Int. Ed.* **50**, 12214-12217 (2011).
62. Horvath, P.; Sebej, P.; Solomek, T.; Klan, P. Small-molecule fluorophores with large Stokes shifts: 9-iminopyronin analogues as clickable tags. *J. Org. Chem.* **80**, 1299-1311 (2015).
63. Kim, E.; Lee, Y.; Lee, S.; Park, S. B. Discovery, understanding, and bioapplication of organic fluorophore: a case study with an indolizine-based novel fluorophore, Seoul-Fluor. *Acc. Chem. Res.* **48**, 538-547 (2015).
64. Goncalves, M. S. Fluorescent labeling of biomolecules with organic probes. *Chem. Rev.* **109**, 190-212 (2009).
65. Li, J.; Wang, J.; Li, H.; Song, N.; Wang, D.; Tang, B. Z. Supramolecular materials based on AIE luminogens (AIEgens): construction and applications. *Chem. Soc. Rev.* **49**, 1144-1172 (2020).
66. Jiang, M.; Gu, X.; Lam, J. W. Y.; Zhang, Y.; Kwok, R. T. K.; Wong, K. S.; Tang, B. Z. Two-photon AIE bio-probe with large Stokes shift for specific imaging of lipid droplets. *Chem. Sci.* **8**, 5440-5446 (2017).
67. Gollnick, K.; Griesbeck, A. Singlet oxygen photooxygenation of furans. *Tetrahedron* **41**, 2057-2068 (1985).
68. Tao, T.; Ma, B. B.; Peng, Y. X.; Wang, X. X.; Huang, W.; You, X. Z. Asymmetrical/symmetrical D-π-A/D-π-D thiazole-containing aromatic heterocyclic fluorescent compounds having the same triphenylamino chromophores. *J. Org. Chem.* **78**, 8669-8679 (2013).

Acknowledgments

This work was supported by the NSFC (22071062, 21871096, 22001077), the Ministry of Science and Technology of the People's Republic of China (2016YFA0602900), Guangdong Science and Technology Department (2018B030308007, 2018A030310359). Prof. Jiangshan Chen of South China University of Technology and Prof. Zheng Zhao of Southeast University were appreciated for their kind help and useful suggestions.

Author contributions

#Y. C. performing the optimization, investigating the scope of the substrate, doing the most experiments on oligomer synthesis and reaction mechanism investigation, Y. C. writing the Original Draft. S. Z. and T. C. Revising – Review & Editing. S. Z. designed & directed the whole project. All authors analyzed the results and commented on the manuscript.

Additional information

Supplementary Information accompanies this paper at:

Competing financial interests

The authors declare no competing financial interests

Table of Contents:

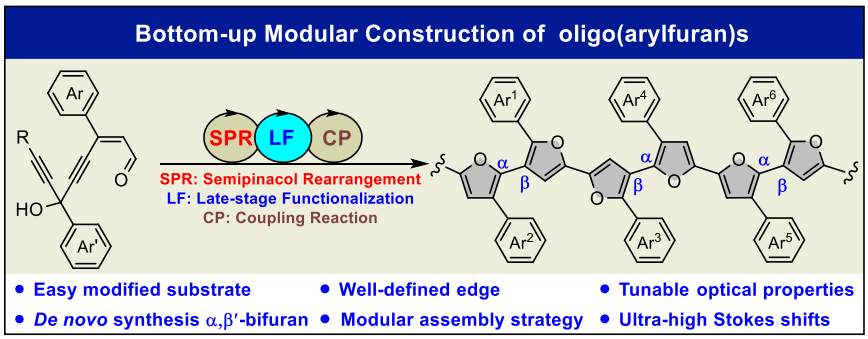

Figures

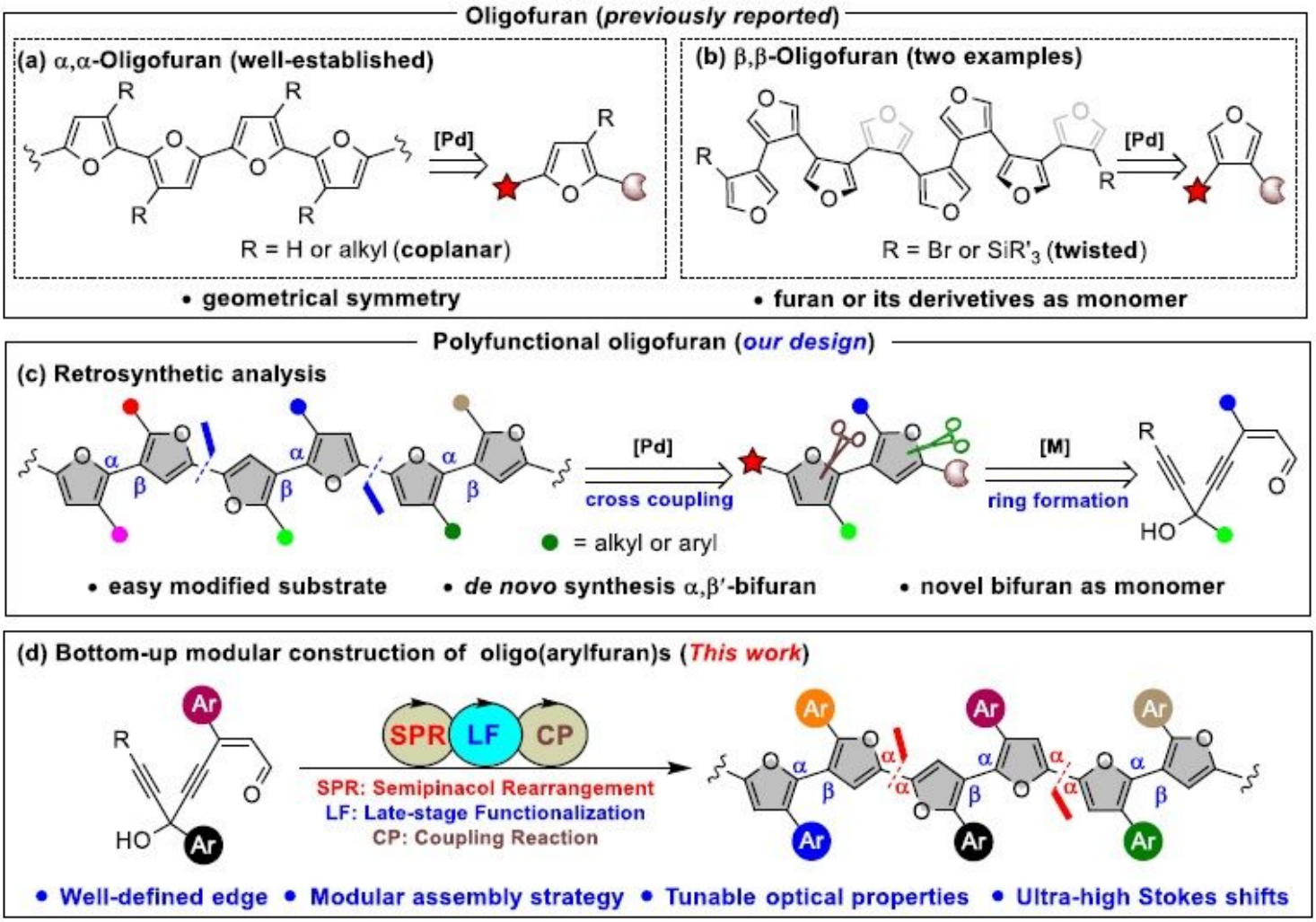

Figure 1

Development of oligofurans. a α,α-oligofurans. b β,β-oligofurans. c retrosynthetic analysis of polyfunctional oligofuran. d This work: bottom-up modular synthesis of oligo(arylfuran)s.

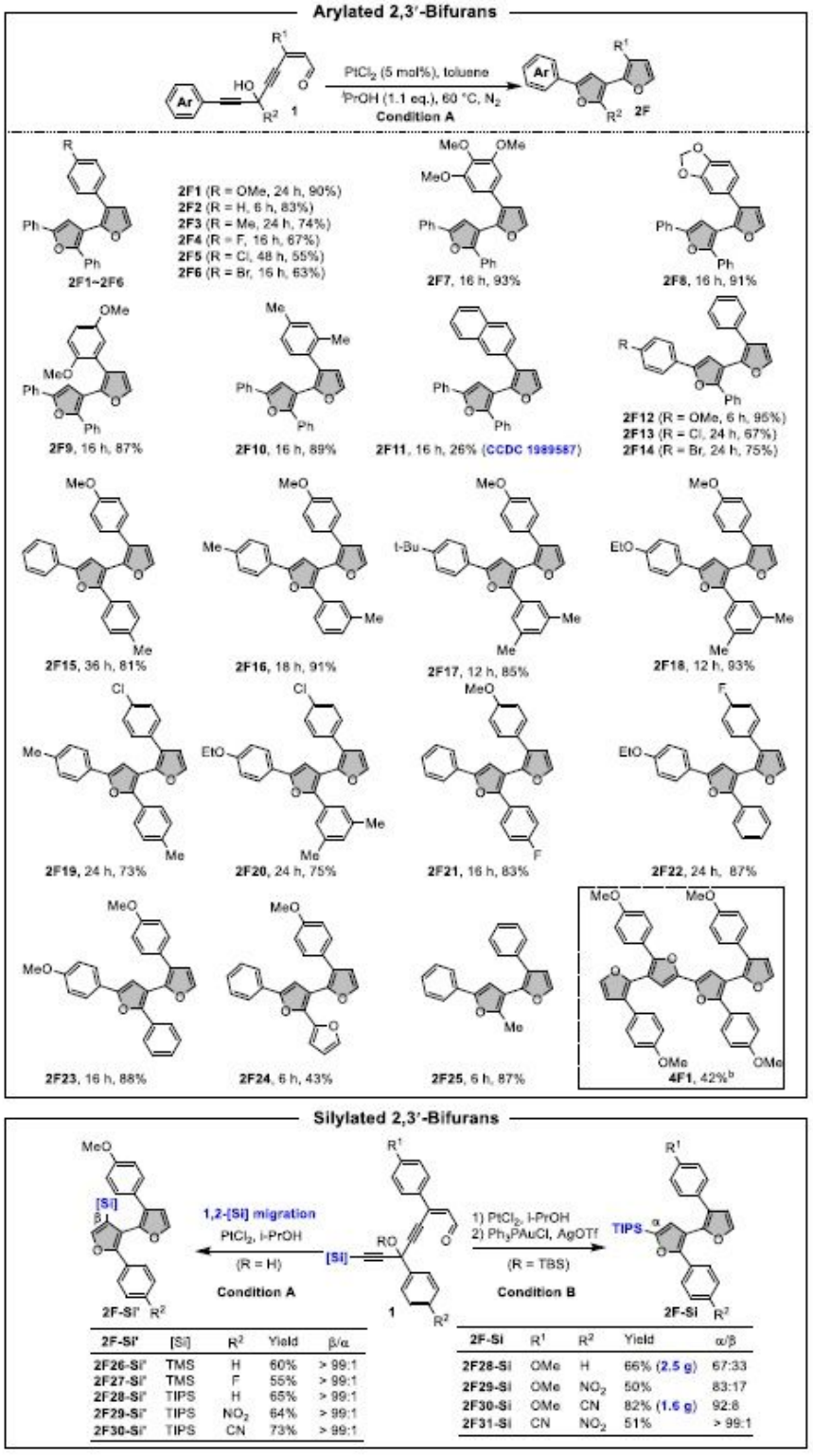

2F-Si′	[Si]	R²	Yield	β/α
2F26-Si′	TMS	H	60%	> 99:1
2F27-Si′	TMS	F	55%	> 99:1
2F28-Si′	TIPS	H	65%	> 99:1
2F29-Si′	TIPS	NO_2	64%	> 99:1
2F30-Si′	TIPS	CN	73%	> 99:1

2F-Si	R¹	R²	Yield	α/β
2F28-Si	OMe	H	66% (2.5 g)	67:33
2F29-Si	OMe	NO_2	50%	83:17
2F30-Si	OMe	CN	82% (1.6 g)	92:8
2F31-Si	CN	NO_2	51%	> 99:1

Figure 2

Substrate scope. aUnless otherwise noted, the reactions were carried out in 0.2 mmol-scale under the standard conditions; bi) PtCl2 (5 mol%), iPrOH (1.1 eq.), toluene, 60 oC; ii) (MeCN)4CuPF6 (5 mol%), toluene, 120 oC; Condition A for 1,2-[Si] migration: PtCl2 (5 mol%), iPrOH (1.1 eq.), toluene, 60 oC; Condition B for the synthesis of α- silyl-bifuran: i) PtCl2 (5 mol%), iPrOH (1.1 eq.), toluene, 60 oC; ii)

PPh3AuCl (5 mol%)/AgOTf (5 mol%), toluene, 90 oC. α/β-regioselectivities were measured based on H1NMR of the crude products.

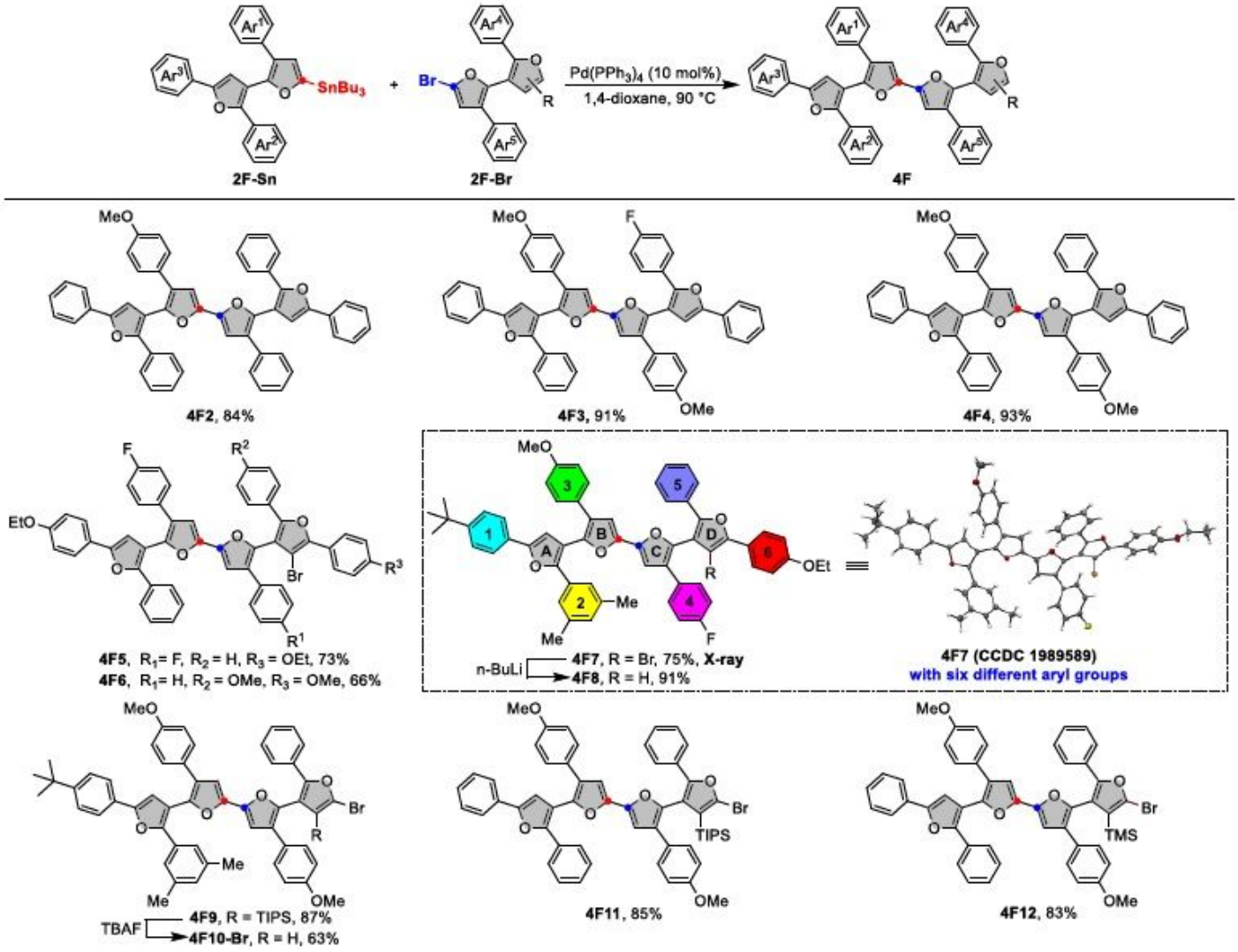

Figure 3

Substrate scope. Stille couping conditions: Pd(PPh3)4 (10 mol%),1,4-dioxane, 90 oC, overnight.

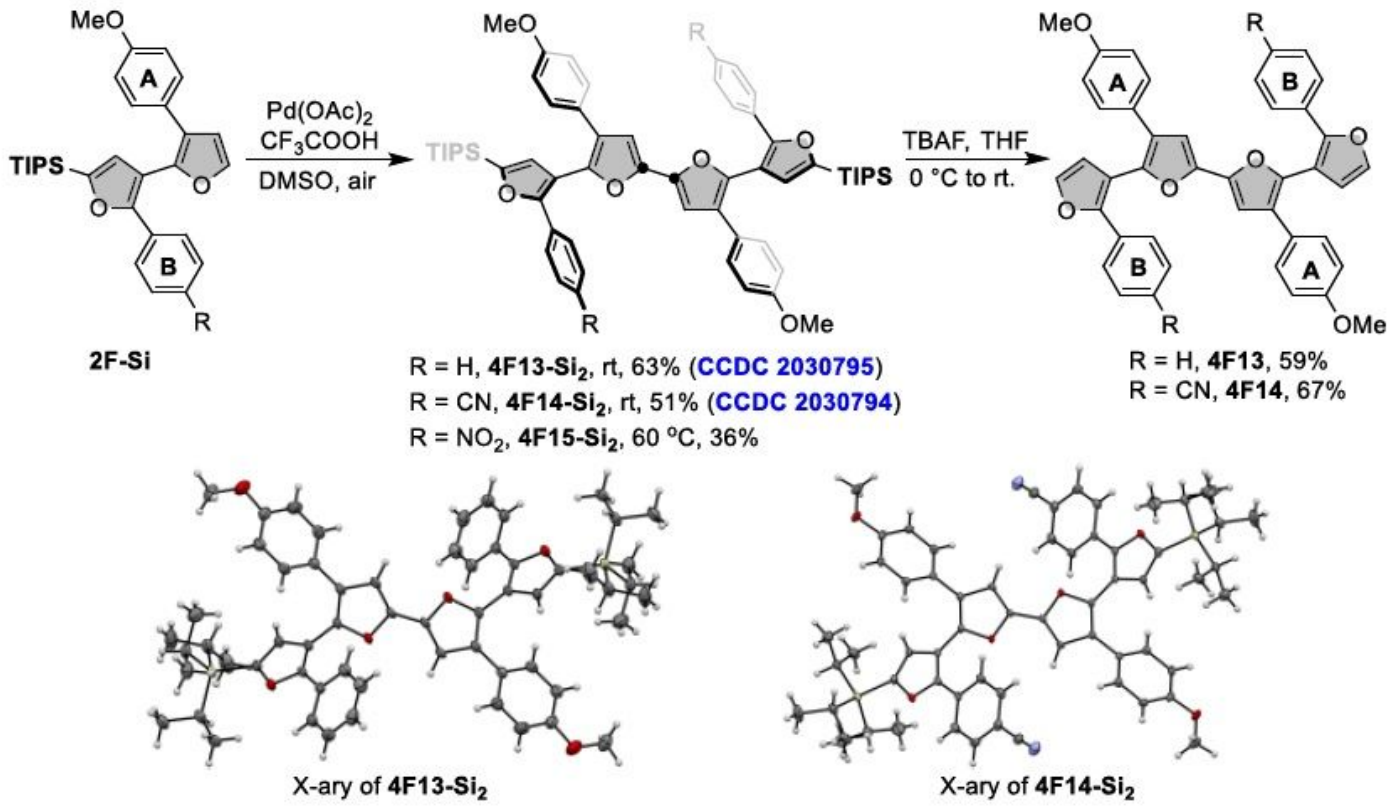

Figure 4

Bottom-up Synthesis of Tetrafuran through Oxidative Homocoupling.

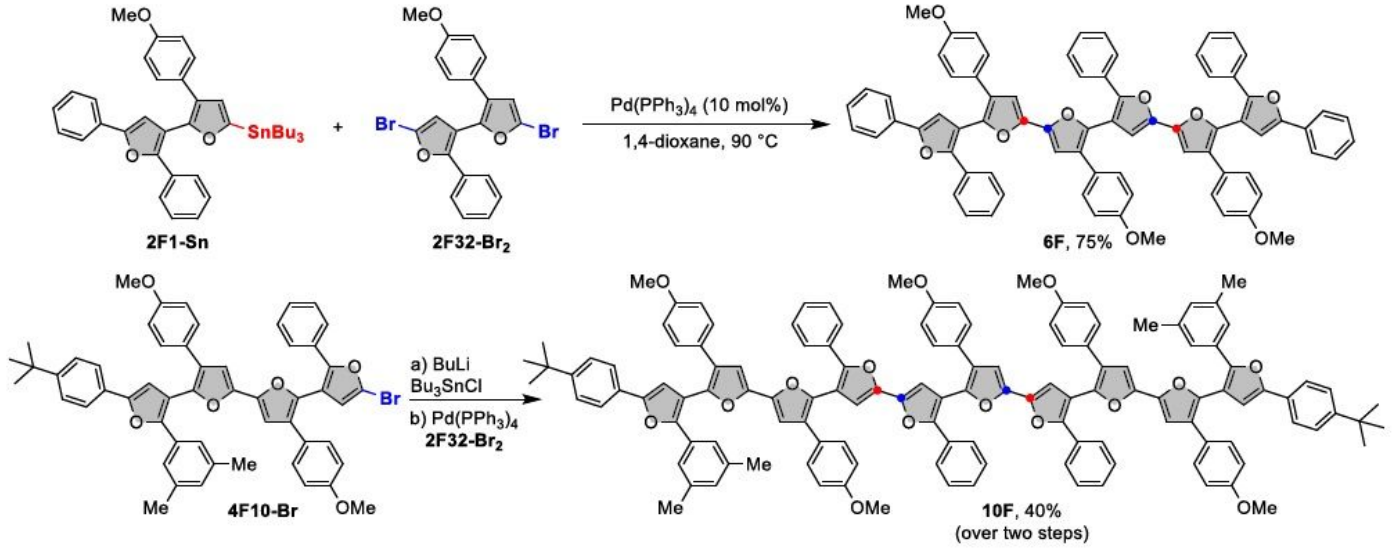

Figure 5

Bottom-up Synthesis of Sexifuran and Decafuran.

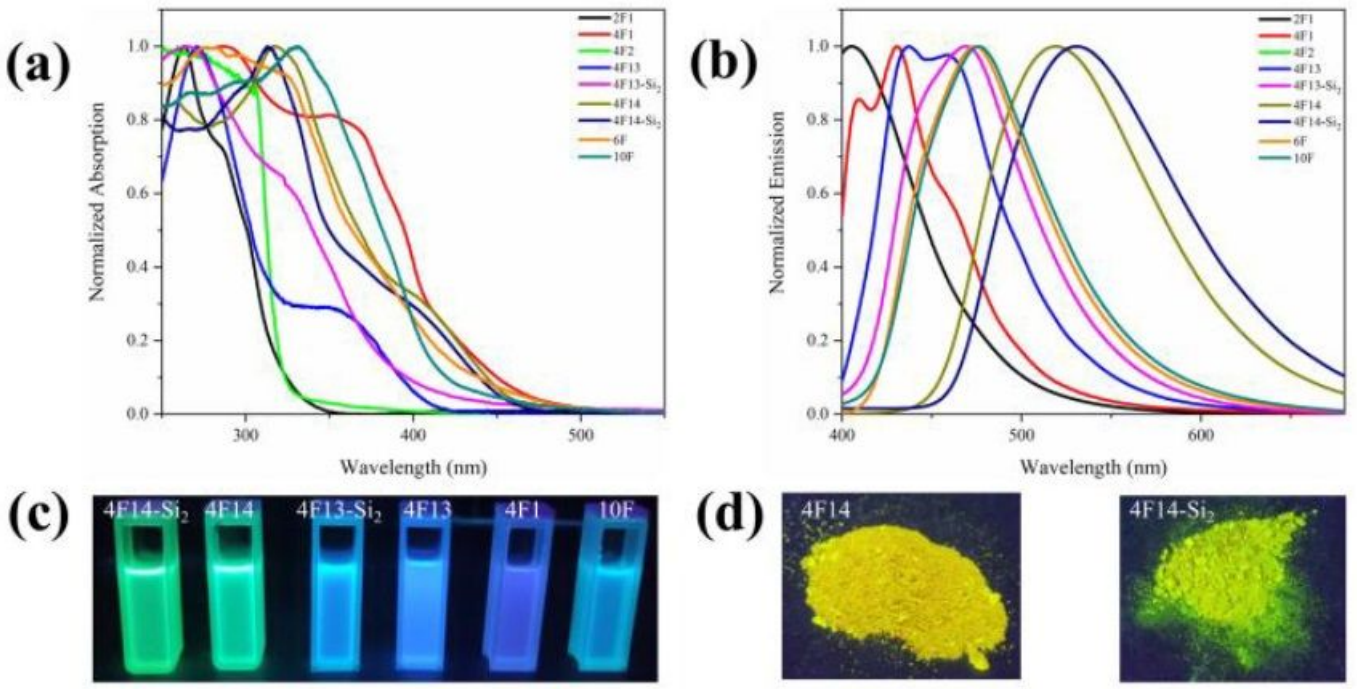

Figure 6

(a) Absorption spectra of representative oligo(arylfuran)s in DCM (Concentration: 10 M). (b) Emission spectra in DCM (ex =365 nm, Concentration: 10 M). (c) Picture of oligo(arylfuran)s in DCM under UV light irradiation (365 nm). (d) Fluorescence image (powder, ex =365 nm).

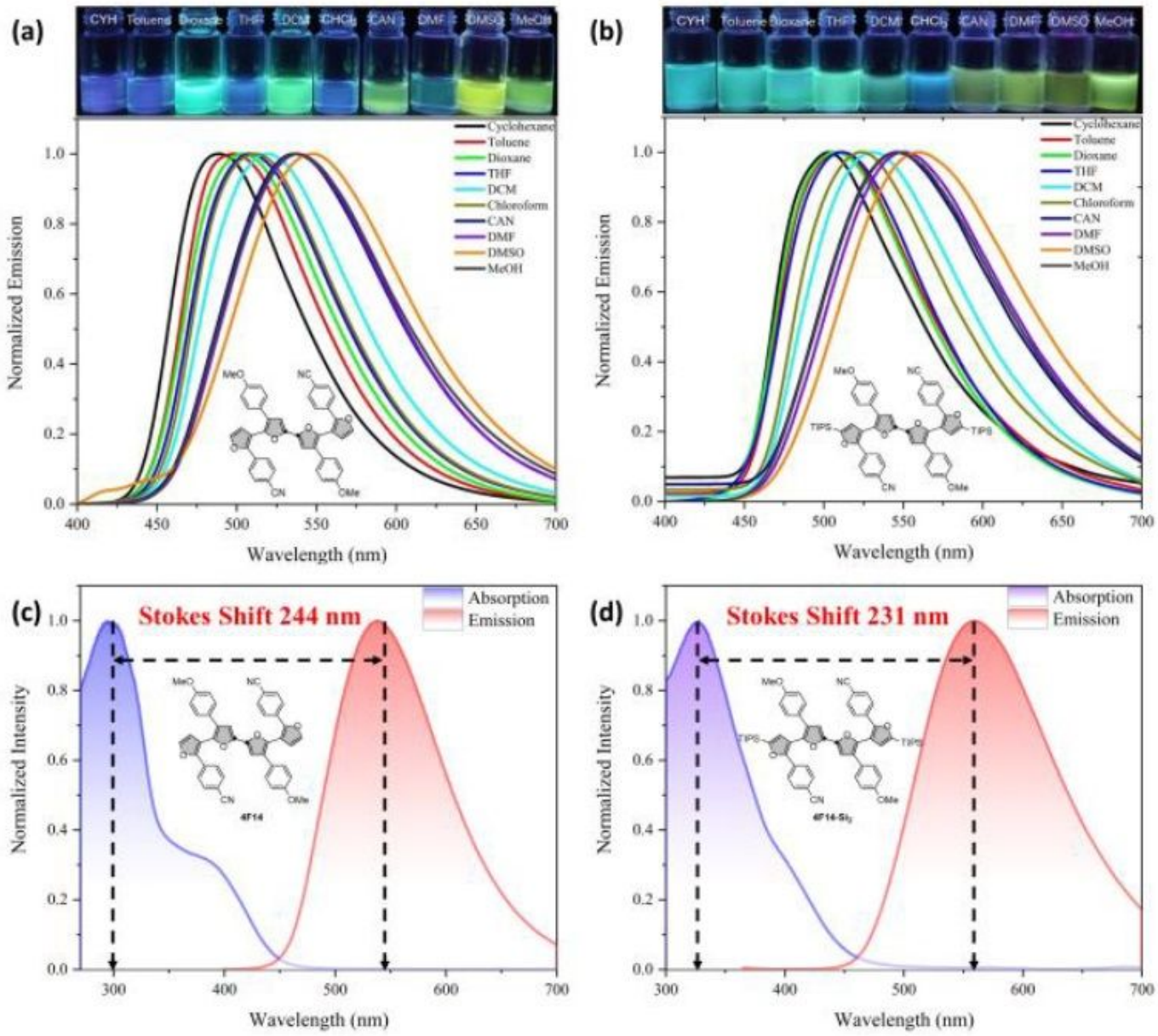

Figure 7

Fluorescence spectra of (a) 4F14 and (b) 4F14-Si2 in solvents of different polarity (THF, tetrahydrofuran; DCM, dichloromethane; CAN, acetonitrile; DMF, N,N- dimethylformamide; DMSO, dimethyl sulfoxide) under 365 nm excitatation. Concentration: 10 uM; Normalized absorption and emission spectra of (c) 4F14 in DMF and (d) 4F14-Si2 in DMSO showing the overlap region.

Supplementary Files

This is a list of supplementary files associated with this preprint. Click to download.

- SupplementaryMaterial.pdf